

Invited Paper ~~~~~

Spectrum Shape and RMS Levels for Simulating Road Vehicle Vibrations

Vincent Rouillard ^{*} and Matthew J. Lamb ^{**}

Abstract

Today, there exists a number of standards designed to assist packaging engineers with implementing suitable laboratory testing regimes for road transport. These standards use vibration spectra that have been shown to often vary significantly from those from measured vibrations. Furthermore, for road transport, these standards protocols do not account for the significant variations in vibration root mean square (rms) levels that are clearly evident during transport as well advocate some form of time-compression to reduce testing duration by artificially amplifying the simulated vibrations. Each of these individual approaches combine to render the simulated vibrations commonly in use around the globe unrepresentative of what occurs during transport, thereby making it difficult to optimise packaging systems. This paper proposes a new approach for simulating road vehicle vibrations that includes five representative spectra based on a large collection of published spectra as well as a risk-based method for determining suitable test intensity – also based on all publicly available rms data.

Keywords: Vehicle vibrations, product damage, protective packaging, vibration spectrum, Power Spectral Density, root-mean-square, Weibull distribution.

1. Introduction

The delicate compromise between the costs (both financial and environmental) related to excessive packaging and those associated with product damage is becoming increasingly important. For this to occur, the prediction of damage rates for various packaging scenarios must be accurate and, to date, this can only be achieved if laboratory simulations of distribution environments - particularly vibrations during transport – are sufficiently accurate. Today, a number of test protocols (as prescribed by ASTM, ISTA, ISO, MIL standards) are aimed at simulating vibrations related to road transport (broadly acknowledged as the most common source of damage to products during the distribution phase) in laboratory settings. Although these protocols have evolved over a number of years, their development and formulation have not, however, always been sound and many such laboratory test protocols remain reliant on flawed assumptions and limited understanding of frequency and statistical analysis techniques [1]. The three main ingredient for simulation of random transport vibrations are: 1) their frequency structure – usually presented as the Power Density Spectrum (PDS); 2) the level at which the vibrations are to be generated – usually by defining the overall root-mean-square (rms) level or its distribution and 3) the duration of the simulation. This paper is based upon two recent publications [2,3] by the authors and brings together the conclusions to form a single, practical approach to simulate more realistic road transport vibrations for packaging optimisation.

^{*} Ph.D, M.Eng, FIEAust, Victoria University, Melbourne, Australia, vincent.rouillard@vu.edu.au

^{**} Ph.D, Victoria University, Melbourne, Australia

1.1. PDS shape

In the main, road vehicle vibrations are predominantly random due to the random nature of road profiles. However, non-random components mainly drive-train vibrations (fixed and varying frequency sinusoids) as well as occasional structural vibrations (when severe road surface aberrations are encountered) can sometime occur and these cannot be properly represented by the PDS [4]. The shape of the PDS is primarily a function of the vehicle's dynamic parameters (suspension type and payload) whereas speed and road roughness are overwhelmingly responsible for the level of the vibrations and, if (near) linear behaviour is assumed, have little influence on the shape of the PDS. Rouillard et al. [1, 3] provide a detailed review of the evolution of the PDS used for transport simulation testing – Fig. 1 – some of which continue to be used around the globe. The majority of the numerous studies that have been published on the topic clearly show that measured PDS often vary significantly from what standards organisations recommend [1]. Despite numerous studies into vibration PDS from road transport vehicles, there has, to date, been no rigorous attempt at comparing the shape of the PDS and relate it to the various types of vehicles and payload conditions. The need was fulfilled by a recent study [PDS paper] the outcomes of which are presented herein and in which a total of 129 PDs were analysed.

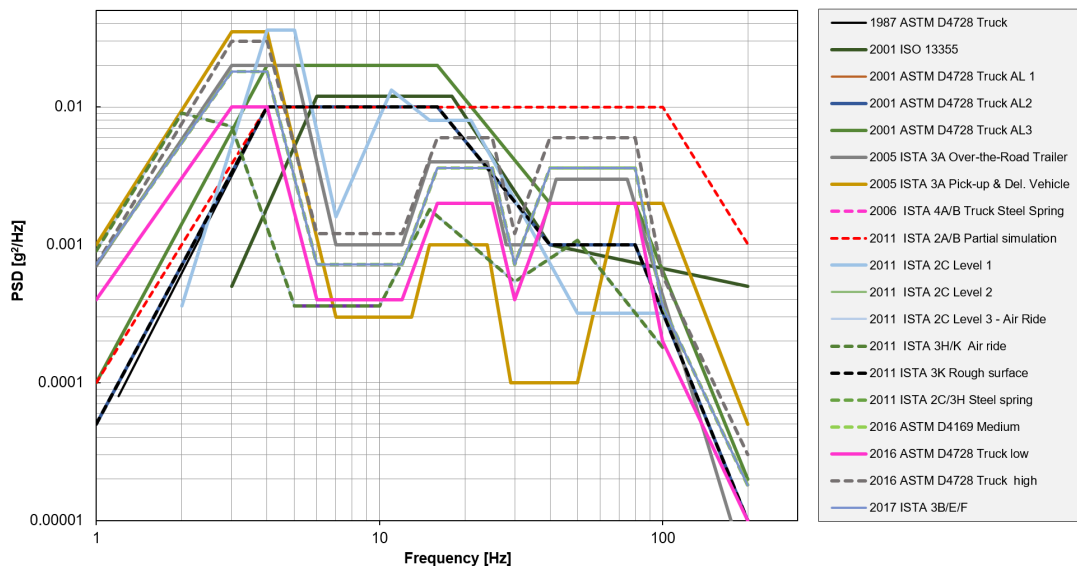


Figure 1. A comprehensive range of Truck PDS including from the original release of ASTM standard D4728 in 1987.

1.2. RMS level

Rouillard and Lamb [2] published a critical literature review on the parameters that influence rms levels of road vehicle vibrations. Since the introduction of powerful and easy-to-use vibration data recorders in the early 1990s, a significant number of studies have been undertaken to characterise specific distribution environments using various vehicle types and configurations and road types [2]. These works, all focus on various aspects of road vehicle vibrations and report a variety of findings including the vibration spectra and the rms levels specific to the conditions of their research. These papers were examined to extract reported vertical rms vibration levels and pertinent associated information (i.e. vehicle type, suspension type, payload, vehicle weight capacity and road type) with the aim of collating the most comprehensive set of published road vehicle vibrations rms values as possible. In addition to the 138 published mean rms levels, 32 values from vibration data previously measured but unpublished by the authors were added to the set making a total of 170 mean rms values representing the broadest range of road transport conditions collated to date.

2. Aim

The aim of this paper is to propose a laboratory test protocol that includes alternative vibration response spectra as well as a practical risk-based approach to select the mean rms level to be selected as well as, if desired, the equivalent rms distribution to be used.

3. Methodology

The approach taken in this paper was treat all data retrieved from all available publications as a global sample to explore the inherent nature of the vertical (heave) vibration response of road transport vehicles.

3.1. PDS shape

The PDS were analysed to establish if they could be grouped in accordance with important vehicle characteristics namely suspension type and payload with the aim of producing a number of archetypal PDS that could be used to represent common vehicle configurations and their corresponding vibration response PDS. This was achieved by matching (curve-fitting) the vibration response PDS with a linear quarter-car model. In this paper, the well-established road elevation profile PDS as described in ISO standard 8608 was used:

$$G_x(n) = G_x(n_o) \cdot \left(\frac{n}{n_o} \right)^{-w} \quad (1)$$

where $G_x(n)$ is the elevation PSD (m^3), n is the spatial frequency (1 cycle/m), n_o is the reference spatial frequency (1 cycle/m) and w is the spectral exponent (usually set at two according to the standard). The magnitude Frequency Response Function (FRF or transmissibility), $T(f)$, of a quarter-vehicle (that is a single-wheeled vehicle) as a function of frequency in Hz travelling at a constant speed, v (m/s), on a road with a an elevation PDS, $G_x(n_o)$, can be estimated from the vertical acceleration response PDS, $R_{\ddot{x}}(f)$, as follows:

$$T(f) = \frac{\sqrt{R_{\ddot{x}}(f)}}{\sqrt{G_{\ddot{x}}(f)}} = \frac{\sqrt{R_{\ddot{x}}(f)}}{\sqrt{G_x(n_o)}} \frac{f^{\left(\frac{w}{2}-2\right)}}{(2\pi)^2 (n_o)^{\frac{w}{2}} v^{\frac{w}{2}}} \quad \text{where } T(f \rightarrow 0) \rightarrow 1 \quad (2)$$

where $G_{\ddot{x}}(f)$ is the acceleration PDS of the pavement surface profile obtainable by differentiating $G_x(f)$. However, $G_x(f)$ can only be known by converting $G_x(n_o)$ to the temporal domain by combining it with the vehicle velocity, v , which, in this case, is not known. However, due to the fractal nature of $G_x(n_o)$, its conversion to the temporal domain – which effectively shifts the PDS to the right with increasing values of v – results in an equivalent rise in the PSD values as illustrated in Fig. 2. This feature offers a work-around by introducing an effective overall road roughness $\hat{G}_x(f_o)$ such that the transmissibility function, $T(f)$, approaches unity at zero Hz. In this paper, measured vibration response PDS were combined with the road acceleration PDS to produce an estimate of the quarter-car magnitude FRF. This FRF was then modelled (fitted using regression) by the theoretical sprung-mass FRF of a 2 degree-of-freedom system described in the Laplace domain as shown in (3).

$$|FRF| = T(s) = \left| \frac{\omega_{n,u}^2 (2\zeta_s \omega_{n,s} s + \omega_{n,s}^2)}{(s^2 + 2\rho\zeta_s \omega_{n,s} s + \omega_{n,u}^2 + \rho\omega_{n,s}^2)(s^2 + 2\zeta_s \omega_{n,s} s + \omega_{n,s}^2) - \rho(2\zeta_s \omega_{n,s} s + \omega_{n,s}^2)^2} \right| \quad (3)$$

Where $\omega_{n,s}$ and $\omega_{n,u}$ are the uncoupled sprung and unsprung mass natural frequencies respectively in rad/s; ζ_s is the sprung mass uncoupled damping ratio (tyre damping is neglected); ρ is the sprung to unsprung mass ratio and $s = \pm i\omega$ is the Laplace operator where ω is the excitation frequency in rad/s. Although the value of the spectral exponent w may, in practice, vary (generally between 2.0 and 2.4), Rouillard and Lamb found that its influence on the prediction of the response PDS was negligible [3].

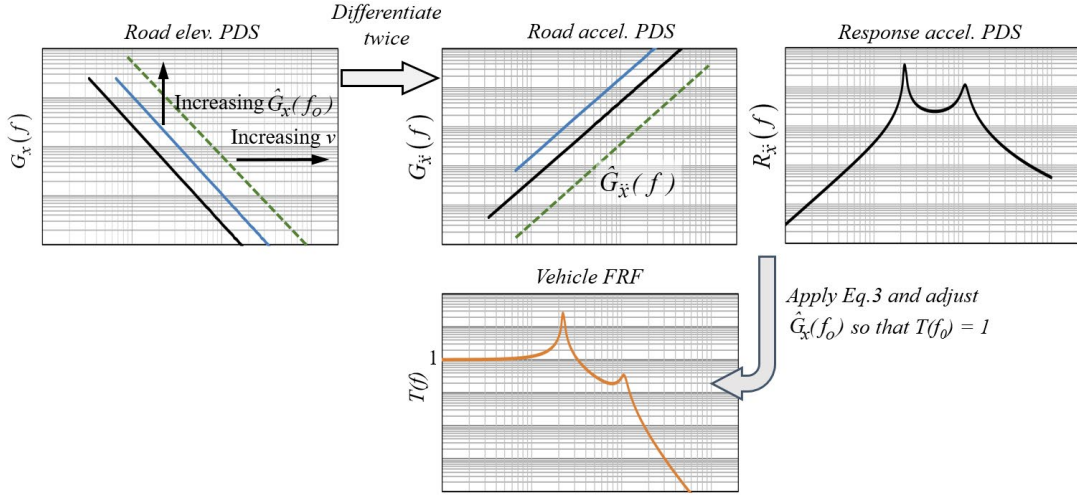


Figure 2. Effect of vehicle speed on the road elevation spectrum (top left) and resulting quarter-car transmissibility (bottom) by iteratively adjusting the road roughness.

3.2. RMS level

The complete set of mean rms values was treated as a random sample that is statistically representative of mean rms vibration levels for road transport in general.

3.2.1. Data classification

To allow for the analysis of parameters which may influence road transport vibration levels, the mean rms data set was categorised into three groups: **Payload**: below or above 50% capacity (due to a lack of detailed information in most publications); **Suspension type**: Steel leaf or Air; **Road type**: Minor roads (metropolitan and minor roads) or Major roads (main roads, arterial roads, highways and motorways).

3.2.2. Analysis Method

Once the rms values were categorised, a statistical analysis process to characterise the rms levels was established. This process was based on the work of Rouillard and Lamb [2] who demonstrated that the probability density function describing the statistical distribution of the vibration levels of vehicles travelling on sealed roads can be adequately defined using a three parameter Weibull function (density) with the shape parameter set to two:

$$p(x) = \frac{2}{\eta^2} (x - x_0) \cdot \exp \left[- \left(\frac{x - x_0}{\eta} \right)^2 \right] \quad \forall \begin{cases} x \in \square \\ x_0 \leq x < \infty \\ \eta \in \square^+ \end{cases} \quad (5)$$

, where: $p(x)$ is the probability density, η is the scale parameter and x_0 is the location parameter.

The authors [5] were also able to establish relationships between the mean heave acceleration rms of the vibration records and the scale and location parameters. These relationships allow for the prediction of the overall rms distribution which enables the range and maximum expected rms level to be estimated. In this study, the cumulative Weibull distribution (6) was used to describe the statistical distribution of reported mean rms levels for the entire mean rms data set as well as mean rms data sets based on the aforementioned categories. The Weibull parameter values were obtained by finding the curve of best fit which allowed each data grouping to be compared at specific values of probability.

$$P(x) = 1 - \exp \left[- \left(\frac{x - x_0}{\eta} \right)^\beta \right] \quad \forall \begin{cases} x \in \square \\ x_0 \leq x < \infty \\ \eta \in \square^+ \end{cases} \quad (6)$$

where β is known as the shape parameter. Following this analysis, the relationships established by Rouillard and Lamb [5] were used to predict the rms distribution associated with a particular combination of transport parameters (suspension type, road type and payload) and risk level.

4. Results

4.1. PSD shape

The analysis herein is based on some 129 PDS computed from a variety of vehicle and road surface configurations. 56 PDS were computed using vibration data measured by the authors over the past 25 years and 73 extracted from published data. A comprehensive summary of the completed data set including sources is freely available through this [link](#):¹⁾

4.1.1. Data classification

The data was classified in two broad sets: 1) Steel leaf suspension and 2) Air ride suspension. Due to challenges in obtaining reliable payload and capacity information for all cases, PDS were classified on the value of the first (sprung mass) natural frequency which is a function of payload and stiffness. Purpose-designed code was implemented to extract the natural frequency of each acceleration response PDS for the two sets namely steel leaf spring and air ride and compute their statistical distributions. The bin width of the statistical distributions had to be carefully selected to yield sensible results which are shown in Fig. 3.

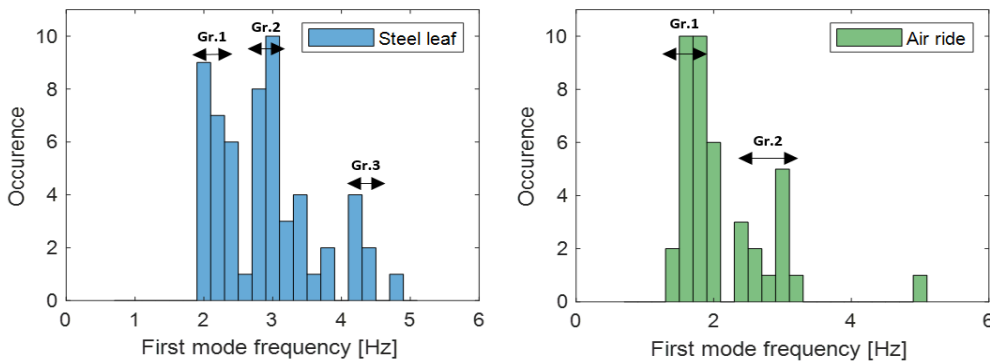


Figure 3. Distribution of first mode (sprung mass) natural frequency for vehicle with steel leaf and air ride suspensions.

4.1.2. Representative spectra

The aim here is to establish a single archetypal of overall PDS to represent each of the five categories (groups) listed in Table 1. Although the frequency of the first resonant mode for each category are well grouped, the second mode (axle hop) is not so well-defined and its frequency tends to vary depending on the vehicle's mass and stiffness ratios. It must be noted here that only the shape of the PDS is of interest in the context of this paper and were normalized to produce unity rms across the rigid-body mode frequencies, namely 1 – 30 Hz. Application of a simple average of the PDS is not suitable as it drowns-out the second mode making it challenging when trying to use the mode as a manifestation of a realistic quarter-car vehicle model. Instead, in order to retain the important features of the vibration response PDS (namely the prominent peaks corresponding to the sprung mass and unsprung mass (axle hop) resonances), a quasi-subjective elimination process was applied. First, those PDS determined to be clearly abnormal (such as those with excessively large peaks outside the typical first and second mode frequency bands representing rigid body vibrations) were discarded. The mean of the remaining PDS was then computed and individual PDS with large deviations from the mean across the low (rigid body) frequency bands were progressively eliminated with the mean re-computed after each elimination resulting in the representative PDS for the group. These PDS are shown in Fig. 4 for each of the five groupings.

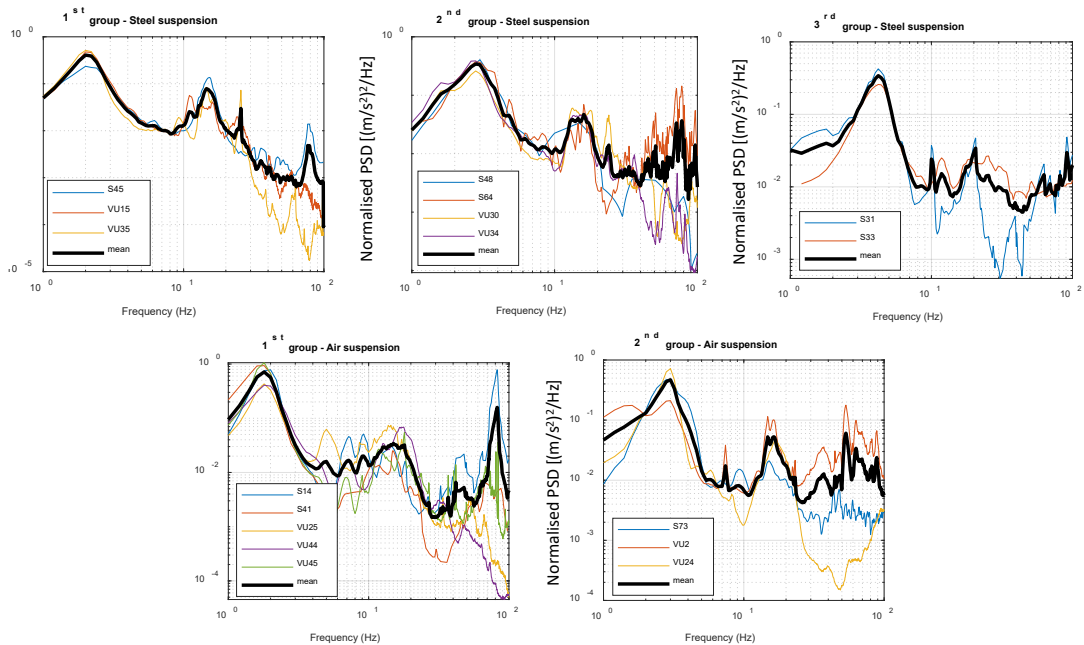


Figure 4. Individual PDS after selective elimination for each of the five groupings along with their mean.

4.1.3. Quarter-car modelling of representative PDS

Each of the five representative PDS (mean PDS from Fig. 5) were combined with the generic road elevation spectrum and fitted to the quarter-car theoretical model (3) to produce estimates of the magnitude FRF. These curve fits yielded the quarter-car modal parameters - Table 1 - for each of the five representative cases for road spectral exponent values of $w = 2.0$ and $w = 2.4$. The PDS fits (normalised to a unit rms) are shown graphically in Fig. 5 where it can be seen that the value of w with the range of 2.0 – 2.4 has no significant influence on the goodness of fit between the calculated and measured PDS.

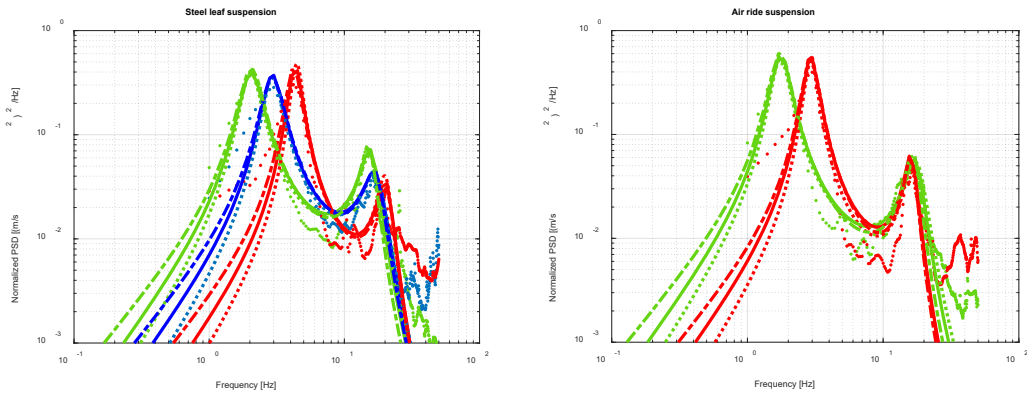


Figure 5. Measured and modelled response PDS for: $w = 2$ (dotted lines); $w = 2.4$ (dash-dot lines) and $w = 2.2$ (solid lines) using parameters from Table 1 for the five representative payload scenarios: Green: Heavy; Blue: Moderate; Red: Light.

Table 1. Quarter-car parameters for $w = 2.0 - 2.4$ with means shown in brackets.

Susp. Type	Payload Level	f_{n_s} [Hz]	f_{n_u} [Hz]	ρ	ζ_s
Steel Leaf	Heavy	2.12 – 2.12 (2.12)	15.2 – 14.9 (15.1)	5.88 – 4.10 (5.00)	0.21 – 0.22 (0.22)
	Moderate	3.16 – 3.10 (3.13)	16.2 – 16.3 (16.3)	4.76 – 3.81 (4.29)	0.21 – 0.23 (0.22)
	Light	4.90 – 4.56 (4.73)	18.4 – 19.2 (18.8)	3.13 – 3.16 (3.15)	0.14 – 0.17 (0.16)
Air Ride	Heavy	1.82 – 1.81 (1.82)	17.2 – 16.3 (16.8)	9.26 – 5.72 (7.49)	0.18 – 0.19 (0.19)
	Light	3.15 – 3.09 (3.12)	15.2 – 15.4 (15.3)	3.70 – 2.97 (3.34)	0.15 – 0.16 (0.16)

4.1.4. Discussion

The results in Fig. 5 also indicate that the higher frequency content of the measured data is not related to rigid body motion but most likely emanate from drivetrain and, in some cases, structural vibrations. As these vibrations are impossible to classify based on vehicle type, it is recommended that the five quarter-car representative spectral models proposed in this paper – namely for steel leaf spring suspended vehicles with heavy, moderate and light loads and air ride type vehicles with heavy and light loads - be used for laboratory simulation for validating packaged systems. It is suggested that, for most packaged product, this is sufficient to test their ability to survive road transport vibrations. These will yield more realistic vibrations than those endorsed by standards organisations and should have a positive impact on the optimisation of packaging designs and a corresponding reduction in packaging waste. The other important observation to be made here is that none of the representative PDS (nor any of the 130 individual PDS) resemble any of the generic spectra used by the various test standards shown in Fig. 1. These latter are over-simplistic and generally fail to feature the significant resonances that occur in reality. Consequently, they tend to produce more broad-banded random vibrations that do not account for the concentration of vibratory energy around the resonances [6].

4.2. RMS level

4.2.1. Entire data set

The distribution of mean rms vibrations for the entire data set - Fig. 6 (a) - shows that, for the vast majority of cases, the mean rms level is contained within the range $0.2 - 3.5 \text{ m/s}^2$. The cumulative distribution of the mean rms level for the entire set is shown in Fig. 6 (b) along with the best-fitting 3-parameter Weibull distribution which can be used to estimate the expected mean rms level for any

specific probability level with the 50th, 75th, 90th and 95th percentiles (denoted as P50, P75, P90 and P95 respectively) highlighted. Such a risk-based approach is aimed at encouraging the pro-active management of vibration levels during distribution and promote the allocation of responsibility and liability if expected or agreed levels of vibrations are exceeded.

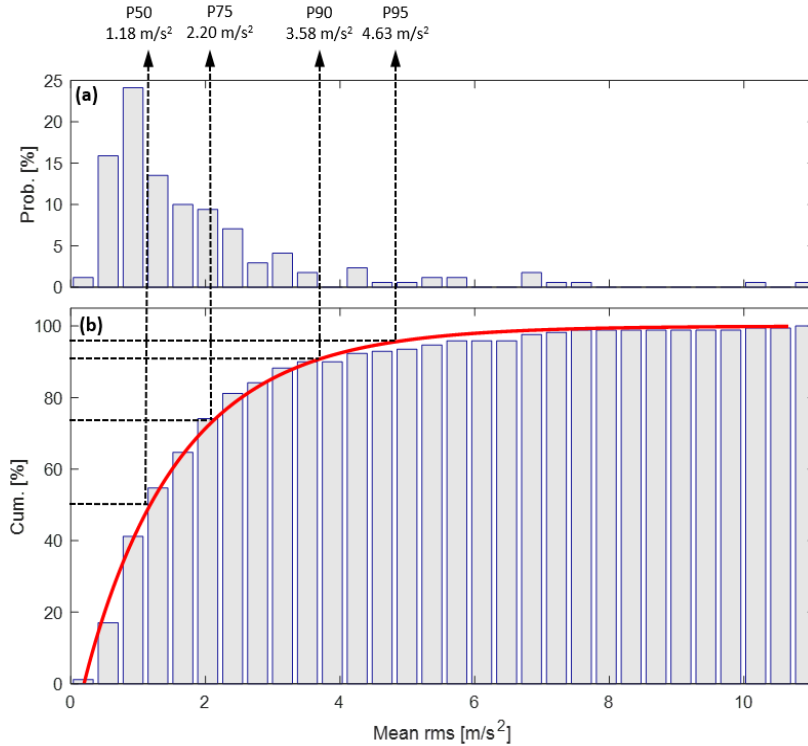


Figure 6: (a) Probability density, (b) cumulative distribution along with the best-fitting Weibull model (red line) of the mean rms vibration level from the entire data set.

4.2.2. Influence of suspension type

The features of the two main types of suspension for commercial vehicles, steel leaf and air ride are briefly discussed in [2]. Although the lower vibration levels afforded by air suspended vehicles is broadly acknowledged, a quantified measure of this advantage over a broad range of vehicles is not available in the literature with the most detailed study to date provided by Singh et al. [7]. The statistical distributions evaluated for the two suspension types are shown in Fig. 7. These were compared with the overall distribution (middle) and a correction function (bottom) calculated using the ratio of the cumulative distributions between the selected data and the entire data set. These correction functions illustrate how suspension type influences mean rms levels as a function of probability of occurrence.

4.2.3. Influence of payload

Broadly, a reduction in load results in an increase in natural frequency hence an increase in overall rms level. In modern air suspension systems, this is mitigated by the automated adjustment of suspension pressure, hence stiffness, to accommodate variations in payload. The statistical distributions for the tow payload classes are shown in Fig. 8. The shift in the mean rms distribution is clear and, when compared with the cumulative distribution for the entire data set, the benefits of heavier payloads on the mean rms levels is plainly evident.

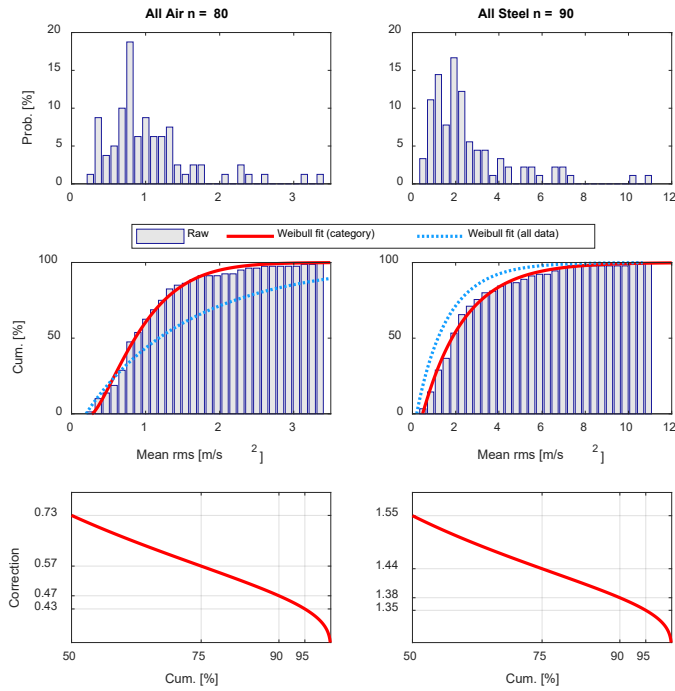


Figure 7: Mean rms probability distribution (top), cumulative distribution (centre) and correction factor (bottom) for all vehicles with air ride (left) and steel leaf (right) suspension.

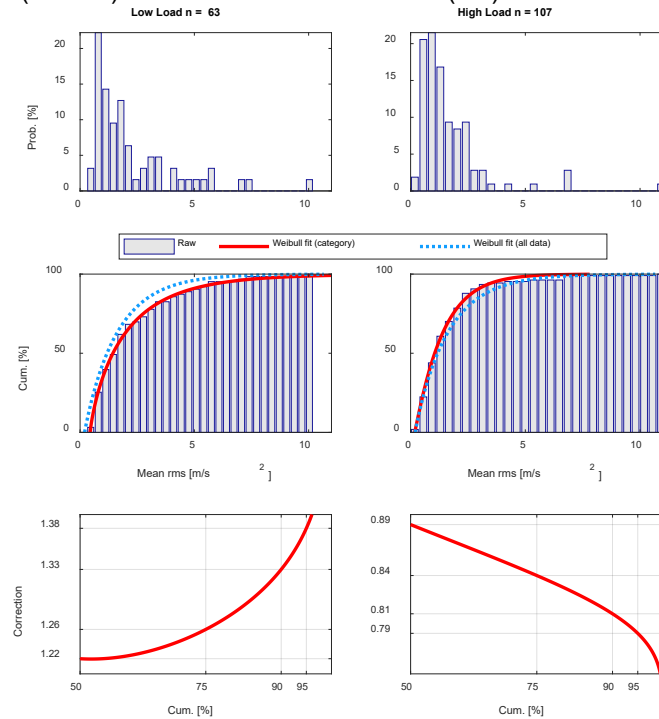


Figure 8: Mean rms probability distribution (top), cumulative distribution (centre) and correction factor (bottom) for all vehicles with low payloads (left) and high payloads (right).

4.2.4. Influence of road type

Given the same vehicle, an increase in speed or road roughness will generally directly increase the heave response. On rough roads this will often be managed by the driver who will adjust the vehicle's speed to suit the rough conditions, whereas, on well-maintained highways and motorways, mean heave rms will be regulated by the speed limit. Due to a lack of detailed information on road roughness and vehicle speed, the mean rms data set was separated into two groups of sealed roads: minor roads (including metropolitan roads) and major roads (incorporating main roads, highways and motorways). Any rms level that was associated with a mix of minor and major road types were excluded from the analysis. Such coarse categorization is bound to contain some overlap but the statistical distributions of the mean rms shown in Fig. 9 show the overall influence of road type on the mean rms level.

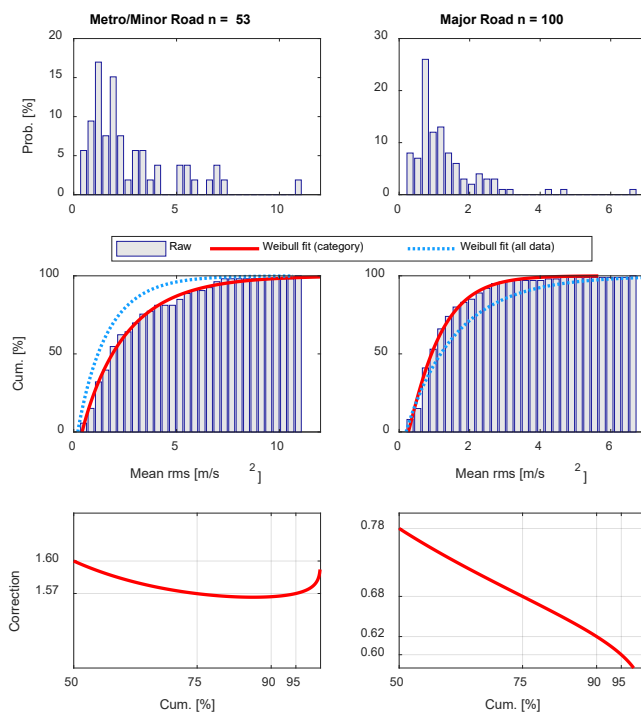


Figure 9: Mean rms probability distribution (top), cumulative distribution (centre) and correction factor (bottom) for all vehicles travelling on minor roads (left) and major roads (right).

4.2.5. Discussion

The influence of suspension type, road type and payload were quantified using the ratio of the Weibull fit of the cumulative distribution function of the categorized data set to the cumulative distribution function of all data. This yielded correction factors based on probability level that can be applied to the statistical distribution of the mean rms level for the entire data set to estimate the combined effect of a variety of transport parameters. Fig. 10 summarizes these correction factors and Table 2 details all possible scenarios for four probability levels and shows how the individual correction factors are combined to calculate the corrected mean rms level for the selected probability levels.

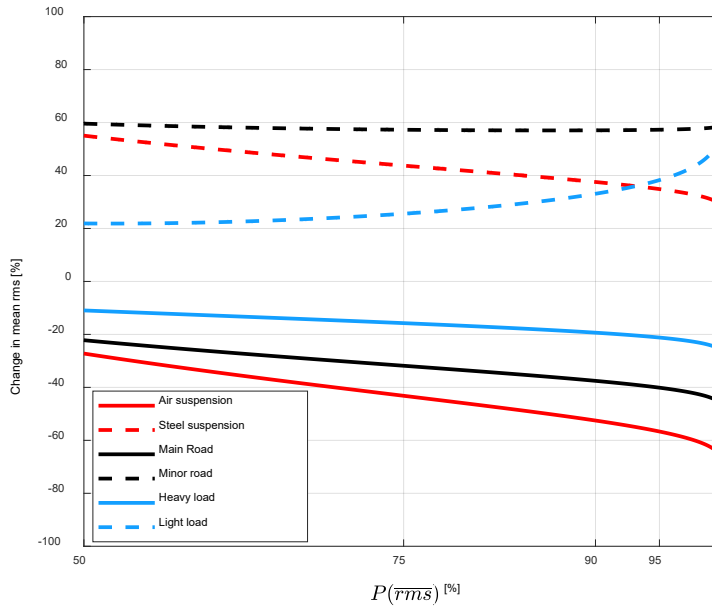


Figure 10: Summary of correction factors to be applied to the statistics of the full data set. Using the results, a risk-based approach for laboratory based vibration testing is recommended as follows:

- [1] Select the probability percentile and record the corresponding expected mean rms based on the entire data set
- [2] Select suspension type
- [3] Select the road type
- [4] Select the payload level
- [5] Use Table 2 to find the combined correction factor.

For example (following the highlighted values in Table 2), for a percentile level of 90% (P90), leaf steel suspension, major road and low payload level, the combined correction factor is 1.14. That is, the expected mean rms level is 1.14 times the expected, P90, mean rms level of the entire (global) data set resulting in a new mean rms of 4.07 m/s².

Once a mean rms value is estimated for the specific journey, the relationships established by Rouillard and Lamb [Weibull paper] can be applied to estimate the distribution of the rms. Direct application of these relationships resulted in a slight underestimate (approximately 4%) of the mean rms. In this study, the equations adjusted to correct for these difference resulting in equations (7) and (8) which were used to estimate the scale and location parameter which can then be used in (5) to estimate the overall rms distribution.

$$\eta = 0.735 \cdot \overline{rms} \quad (7)$$

$$x_o = 1.082 \cdot \overline{rms} - \eta \quad (8)$$

As an illustration, four scenarios for the 90th percentile – P90 – are given in Fig. 11. The four scenarios (taken from Table 1) represent:

- Air ride suspension with high payload on major roads (0.85 m/s² mean rms)
- Air ride suspension with high payload on minor roads (2.14 m/s² mean rms)

- Steel suspension with low payload on major roads (4.07 m/s² mean rms)
- Steel suspension with low payload on minor roads (10.32 m/s² mean rms)

Table 2: Application of correction factors to obtain corrected mean rms values.

	Mean rms [m/s ²]	Suspension Type		Road		Payload		Combined Correction Factor	Corrected mean rms [m/s ²]
P50	1.18	Steel leaf	1.55	Minor	1.60	Low (< 50%)	1.22	3.03	3.57
						High (> 50%)	0.89	2.21	2.60
				Major	0.78	Low (< 50%)	1.22	1.47	1.74
						High (> 50%)	0.89	1.08	1.27
		Air ride	0.73	Minor	1.60	Low (< 50%)	1.22	1.42	1.68
						High (> 50%)	0.89	1.04	1.23
				Major	0.78	Low (< 50%)	1.22	0.69	0.82
						High (> 50%)	0.89	0.51	0.60
P75	2.20	Steel leaf	1.44	Minor	1.57	Low (< 50%)	1.26	2.85	6.27
						High (> 50%)	0.84	1.90	4.18
				Major	0.68	Low (< 50%)	1.26	1.23	2.71
						High (> 50%)	0.84	0.82	1.81
		Air ride	0.57	Minor	1.57	Low (< 50%)	1.26	1.13	2.48
						High (> 50%)	0.84	0.75	1.65
				Major	0.68	Low (< 50%)	1.26	0.49	1.07
						High (> 50%)	0.84	0.33	0.72
P90	3.58	Steel leaf	1.38	Minor	1.57	Low (< 50%)	1.33	2.88	10.32
						High (> 50%)	0.81	1.75	6.28
				Major	0.62	Low (< 50%)	1.33	1.14	4.07
						High (> 50%)	0.81	0.69	2.48
		Air ride	0.47	Minor	1.57	Low (< 50%)	1.33	0.98	3.51
						High (> 50%)	0.81	0.60	2.14
				Major	0.62	Low (< 50%)	1.33	0.39	1.39
						High (> 50%)	0.81	0.24	0.85
P95	4.63	Steel leaf	1.35	Minor	1.57	Low (< 50%)	1.44	3.05	14.13
						High (> 50%)	0.79	1.67	7.75
				Major	0.60	Low (< 50%)	1.44	1.17	5.40
						High (> 50%)	0.79	0.64	2.96
		Air ride	0.43	Minor	1.57	Low (< 50%)	1.44	0.97	4.50
						High (> 50%)	0.79	0.53	2.47
				Major	0.60	Low (< 50%)	1.44	0.37	1.72
						High (> 50%)	0.79	0.20	0.94

Such distributions can be used to make risk-based decisions as to the maximum rms level expected for a particular road transport scenario and its probability of occurrence. In practical terms, costs associated with protective packaging (material, transport volume, disposal costs etc.) can be optimized against the costs associated with product damage. It is acknowledged that there may be some variation in the roughness associated with major and minor roads from different regions in the world and minor adjustments to the mean rms may be required. For these instances Múčka [***] has compiled a valuable reference for comparing the roughness levels of various road types around the world.

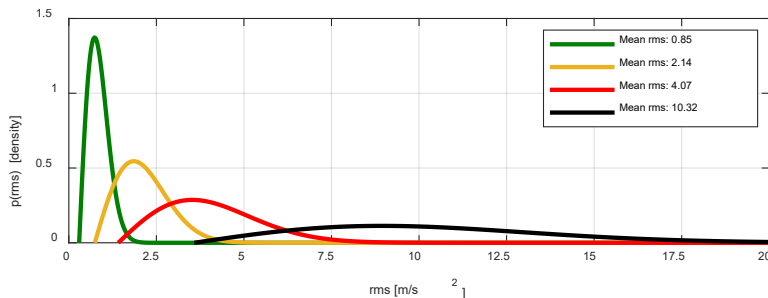


Figure 11: Probability density function (top) and cumulative distribution (bottom) for a range of mean rms values corresponding to the percentile level of 90% (see Table 2).

5. Conclusion

Analysis of an extensive collection of vibration response data measured from a broad range of heavy goods road vehicles resulted in five archetypal response PDS (three for steel leaf suspension and two for air ride suspension) that can be considered as representative response PDS for the rigid body response of road transport vehicles. It is recommended that these five representative spectra be used to evaluate and optimise the vibration resistance of products during road transport. These will yield more realistic vibrations than those promoted by standards organisations and should have a positive impact on the optimisation of packaging designs and a corresponding reduction in packaging waste. It is important to note that these spectra only describe rigid-body vibrations and do not include discrete frequency vibrations (of fixed or varying frequencies) that are caused by other sources such as the drivetrain.

A total of 170 mean rms values were analysed statistically to reveal the influence of some important parameters namely, suspension type, road type and payload. The three-parameter Weibull distribution was used to characterize the cumulative distribution functions for each scenario and was subsequently used to calculate correction factors as a function of mean rms probability level. The results enable the application of a risk-based approach to estimating the mean rms level for any road transport scenario based on the three aforementioned parameters. Finally, to account for the fact that the mean rms vibration is not, by itself, sufficient to completely describe vibration levels during road transport, the range of rms level expected to exist is predicted using a model based on the three-parameter Weibull distribution as a function of mean rms level. This model can be used to determine the expected maximum rms level to occur for any specific road transport scenario thus enabling the optimisation of protective packaging.

5.1.1. Acknowledgment

The authors would like to acknowledge the support of the Victorian Higher Education State Investment Fund and Victoria University as well as Mr. K. Paudel for his assistance in managing the vibration data set.

6. References

1. Rouillard, V., Lamb M.J., Lepine J., Long M. and Ainalis D. "The case for reviewing laboratory-based road transport simulations for packaging optimisation." *PTS* 34, no. 6 (2021): 339-351.
2. Lamb M.J., and Rouillard V. "On the parameters that influence road vehicles vibration levels." *PTS* 34, no. 9 (2021): 525-540.
3. Rouillard V. and Lamb M.J., "Characterisation of the Rigid Body Vibration Spectra of Road Transport Vehicles". *PTS* (in press)
4. Randall, R. B. "Frequency analysis." *Naerum (DK): Bruel & Kjaer* (1987).
5. Rouillard, V. and Lamb, M.J. "Using the Weibull distribution to characterise road transport vibration levels." *PTS* 33, no. 7 (2020): 255-266.
6. Rouillard, Vincent. "Generating road vibration test schedules from pavement profiles for packaging optimization." *PTS* 21, no. 8 (2008): 501-514.
7. Singh, J., Singh S.P. and Joneson E. "Measurement and analysis of US truck vibration for leaf spring and air ride suspensions, and development of tests to simulate these conditions." *PTS* 19, no. 6 (2006): 309-323.

1) this [link](#): →

https://onedrive.live.com/edit?id=4D0488759CD2240B!25920&resid=4D0488759CD2240B!25920&ithint=file%2Cxlsx&redeem=aHR0cHM6Ly8xZHJ2Lm1zL3gvcyFBZ3NrMHB4MWIBUk5nY3BBam4tUnBhVXIiWENYX1E_ZT1JUTBmUU8md2RMT1I9YzI0QUU5NzlwLTdBNjctREU0Qy1CNkEwLTYzMjVDRDA5Q0NEQQ&migratedtospo=true&wdLOR=c24AE9720-7A67-DE4C-B6A0-6325CD09CCDA&wdo=2&cid=4d0488759cd2240b

(Received: 1 August 2024)